

# Enumeration of Polyominoes & Polycubes Composed of Magnetic Cubes

Yitong Lu<sup>1</sup>, Anuruddha Bhattacharjee<sup>2</sup>, Daniel Biediger<sup>1</sup>, Min Jun Kim<sup>2</sup>, Aaron T. Becker<sup>1</sup>

**Abstract**—This paper examines a family of designs for magnetic cubes and counts how many configurations are possible for each design as a function of the number of modules. *Magnetic modular cubes* are cubes with magnets arranged on their faces. The magnets are positioned so that each face has either magnetic south or north pole outward. Moreover, we require that the net magnetic moment of the cube passes through the center of opposing faces. These magnetic arrangements enable coupling when cube faces with opposite polarity are brought in close proximity and enable moving the cubes by controlling the orientation of a global magnetic field. This paper investigates the 2D and 3D shapes that can be constructed by magnetic modular cubes, and describes all possible magnet arrangements that obey these rules. We select ten magnetic arrangements and assign a “color” to each of them for ease of visualization and reference. We provide a method to enumerate the number of unique polyominoes and polycubes that can be constructed from a given set of colored cubes. We use this method to enumerate all arrangements for up to 20 modules in 2D and 16 modules in 3D. We provide a motion planner for 2D assembly and through simulations compare which arrangements require fewer movements to generate and which arrangements are more common. Hardware demonstrations explore the self-assembly and disassembly of these modules in 2D and 3D.

## I. INTRODUCTION

Small-scale modular robots are often designed to be manipulated in large groups by an external system. Magnetic forces are a popular choice for manipulating these robots because the robots can be directly controlled simply by incorporating magnets or ferromagnetic material in the robot body. In the last few decades, many research projects have been conducted based on magnetic actuation and coupling systems to explore reconfigurable modular robotics at different length scales [1]–[4]. Researchers have developed modules with excellent locomotion and manipulation abilities, and have integrated advanced control algorithms. Several reconfiguration strategies of modules, such as autonomous and distributed stochastic self-assembly, disassembly, self-reconfiguration by rotation in a planar workspace, locomotion through reconfiguration on a cubic lattice, and universal and distributed reconfiguration planning for square and hexagonal-lattice-based robots have been investigated [5], [6].

Much related work has focused on the “Tilt model” where components move in a straight line until they hit an obstacle, and combine when mating particles are brought close together. Solutions often design workspace obstacles that

This work used HPE DSI/IT computational resources and was supported by the NSF under Grant Nos. [IIS-1553063, IIS-1849303, CNS-1932572].

<sup>1</sup>Authors are with the University of Houston, Houston, TX 77204 USA {ylu36, debiediger, atbecker}@uh.edu.

<sup>2</sup>Authors are with Southern Methodist University, Dallas, TX 75275 USA {abhattacharjee, mjkim}@lyle.smu.edu.

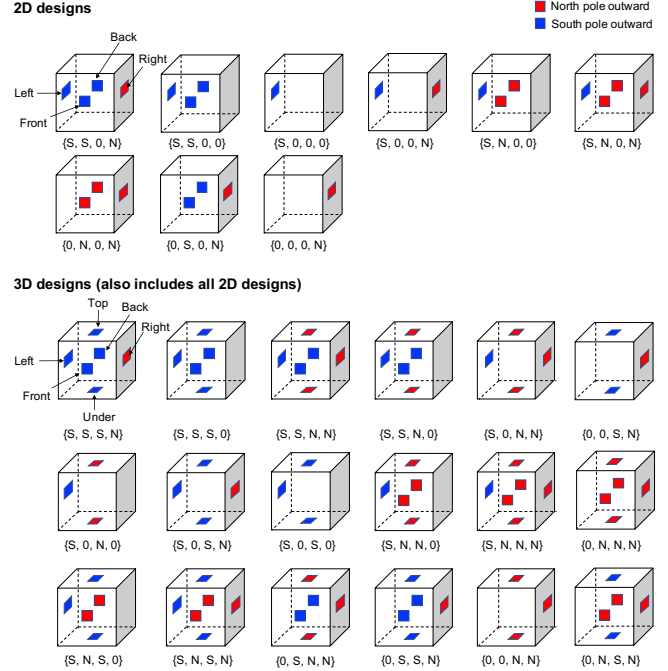


Fig. 1. Designs of 2D and 3D modular cubes. Underneath each cube the arrangement is labeled as {left [L], front [F]/back [B], top [T]/under [U], right [R]}.

enable arbitrary reconfiguration of components pushed by a global force [7], [8]. We designed algorithms that enabled efficient construction of desired shapes [9], and workspace obstacles that enabled sorting and classifying constructed polyominoes [10].

This previous work did not consider the stability or robustness of the structures generated. Recent work in [11], [12] examined the forces between individual components and evaluated if a structure of module robots would be stable — if it would topple or collapse under its own weight, especially during the process of reconfiguration.

Our future goal is to design motion plans for magnetic modular cubes to enable them to form shapes suitable for fast motion, yet with designed fracture points so they can be easily disassembled at a goal and reconfigured into tools or structures. As first steps toward that goal, this paper presents the following contributions: (1) Design and demonstrations of magnetic modular cubes (MMCs) which are simple in design, scalable, and highly reconfigurable through controlled assembly-disassembly. (2) Analysis of all possible magnetization profiles that match the specifications of our modular cubes. (3) A method to count the number of unique configurations for a given set of cubes. (4) Enumerate the unique configurations up to  $n = 20$  in 2D and  $n = 16$  in 3D. (5) Provide a motion planner for 2D assembly.

(6) Monte Carlo simulations to measure the frequency that certain shapes can be constructed and the required number of movement steps to generate the shapes. (7) Conduct hardware experiments that explore the self-assembly and disassembly of these modules in 2D and 3D. For applications of these magnetic cubes, see [13].

## II. DESIGN OF MAGNETIC MODULAR CUBES

We design the MMCs so they can be controlled by a global magnetic field. The cubes are manufactured so they align with an applied magnetic field. The global magnetic field provides a reference frame with a magnetic south to the left and north to the right. We labeled each face of the cube as [L, F, B, T, U, R] for *left*, *front*, *back*, *top*, *under*, and *right* faces. On each face at most one axially magnetized permanent magnet is embedded. Each cube must have a net magnetic orientation. The magnets are positioned with poles facing outwards such that each face is either north or south and such that the net magnetic moment of the cube from magnetic south to north passes through the center of opposing faces. This net magnetic moment is required because it enables “pivot walking” and “rolling” the cubes. Pivot walking is a movement gait that alternately lifts the north or south pole of the cube so the cube balances on the opposing edge, and then applies torque to spin the cube on the balancing edge, as in [14], [15]. The rolling motion [16] can be achieved by applying continuous rotational magnetic torque along an axis perpendicular to the axis of net magnetization of a cube to roll it towards the desired direction.

Because the magnetic field passes through the center of the cube face, the magnetic field must be rotationally symmetric across the left-to-right axis. Thus the magnetization of  $F=B$  and  $T=U$ . We can choose the L to be ( $S$  or  $0$ ), the F and B to be ( $S$ ,  $0$ , or  $N$ ), the T and U to be ( $S$ ,  $0$ , or  $N$ ), and the R ( $0$  or  $N$ ), for a total of  $2 \cdot 3 \cdot 3 \cdot 2 = 36$  arrangements. The arrangement is labeled as  $\{L, F/B, T/U, R\}$ . We then remove the nine arrangements of the form  $\{0, *, *, 0\}$  because they have no net magnetic moment. Therefore, there are 27 sets of suitable magnet arrangements. 2D designs of MMCs only allow connection along the  $x$ -axis and  $y$ -axis. No magnets are embedded on the top [T] or under [U] faces. 3D designs of MMCs enable connection along faces (see Fig. 1).

Due to the MMCs’ cubic design, magnetically connected structures of MMCs are polyominoes in 2D and polycubes in 3D. Polyominoes and polycubes are a classic topic in combinatorics. This paper draws on a rich literature and results on enumerating polyominoes and polycubes [17]–[21] and on coloring them [22]. Work on characterizing upper and lower bounds on the number of polyominoes and polycubes is an active research area [21], [23], and will be relevant to modular robotic construction.

Similarly, there has been a great deal of recent research on how to design workspaces that exploit global control of magnetic particles to design arbitrary shapes [8], [24], [25], and on the complexity of motion planning under such constraints. These papers provide important solutions on how to design workspaces that enable fast rearrangement of cubes,

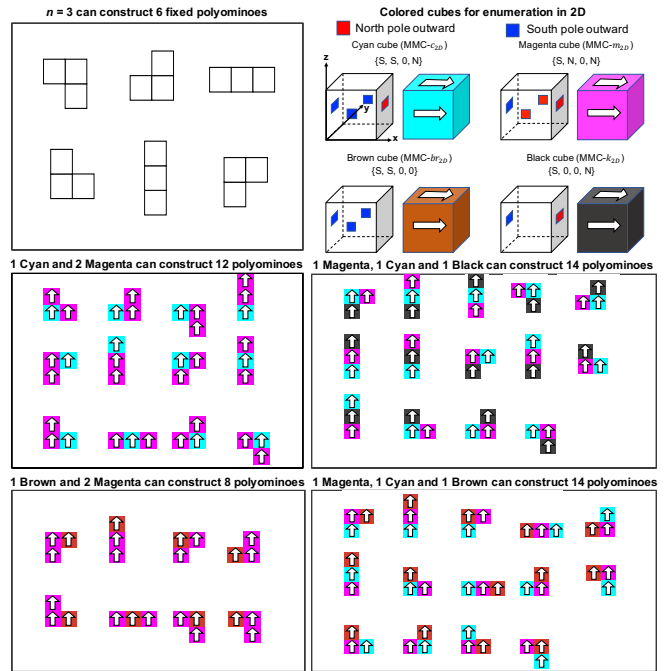


Fig. 2. Enumeration of colored cubes in 2D. The composition of cube types determines the number of polyominoes that can be made. The white arrow indicates the direction of south to north magnetic pole.

but they do not provide insight on how to build those cubes. Moreover, these works tend to assume all cubes will stick together if brought close enough in proximity. In contrast, this paper focuses on the configurations made possible by the magnetic profiles of the cubes.

## III. GENERATE ALL POSSIBLE POLYOMINOES IN 2D

*Polyominoes* are face-connected sets of unit cubes that lie on the square-grid graph. Each cube is represented by an integer tuple  $(x, y)$ . Cubes  $(x_1, y_1)$  and  $(x_2, y_2)$  are adjacent if  $|x_1 - x_2| + |y_1 - y_2| = 1$ . Two *free polyominoes* are considered distinct if they have different shapes, but they cannot be rotations of each other. Two *fixed polyominoes* are considered distinct if they have different shapes or orientations. Because the global magnetic field provides an orientation, we consider fixed polyominoes for our MMCs design. The number of fixed polyominoes of size  $n$  is denoted by  $A_{n,2D}$ . The number of polyominoes grows exponentially [23]

$$\lim_{n \rightarrow \infty} (A_{n,2D})^{\frac{1}{n}} = \lambda. \quad (1)$$

We implemented a method to enumerate the fixed polyominoes and unique colored polyominoes that can be constructed by a set of MMCs [26]. Based on the hardware experiment environment (see Section V), we developed a 2D motion planner using a bounded  $11 \times 11$  workspace that generates the set of valid colored polyominoes reachable by global moves from an initial configuration. The cubes are represented by axis-aligned, unit-length tiles in our motion planner. Arrows on the tiles indicate the direction of the net magnetization (from magnetic south pole to north pole). We select four magnet arrangements that use at least two magnets and, for ease of visualization, assign them the colors cyan, magenta, brown, and black (see Fig. 2 top right).

TABLE I. NUMBER OF FIXED POLYOMINOES  $A_{n,2D}$ , WHERE  $n$  IS THE NUMBER OF CUBES. WITH MMC- $M_{2D}$  AND MMC- $C_{2D}$ ,  $C_{n,i}$  IS THE NUMBER OF COLORED POLYOMINOES WITH  $i$  MAGENTA CUBES AND  $n$  TOTAL CUBES. ROW MAXIMUM IN ORANGE.

$n$	$A_{n,2D}(n)$	$C_{n,0}$ (with 0 magenta cubes)	$C_{n,1}$ (with 1 magenta cube)	$C_{n,2}$ (with 2 magenta cubes)	$C_{n,3}$ (with 3 magenta cubes)	$C_{n,4}$ (with 4 magenta cubes)	$C_{n,5}$ (with 5 magenta cubes)	$C_{n,6}$ (with 6 magenta cubes)	$C_{n,7}$ (with 7 magenta cubes)	$C_{n,8}$ (with 8 magenta cubes)	$C_{n,9}$ (with 9 magenta cubes)	$C_{n,10}$ (with 10 magenta cubes)
1	1	1	1									
2	2	1	4	1								
3	6	1	12	12	1							
4	19	1	26	64	26	1						
5	63	1	46	230	230	46	1					
6	216	1	72	642	1,256	642	72	1				
7	760	1	105	1,505	5,070	5,070	1,505	105	1			
8	2,725	1	146	3,107	16,542	28,166	16,542	3,107	146	1		
9	9,910	1	196	5,828	45,992	122,248	122,248	45,992	5,828	196	1	
10	36,446	1	256	10,163	112,934	440,761	684,848	440,761	112,934	10,163	256	1
11	135,268	1	327	16,745	251,269	1,374,201	3,116,870	3,116,870	1,374,201	251,269	16,745	327
12	505,861	1	410	26,373	516,274	3,810,917	12,049,830	17,549,004	12,049,830	3,810,917	516,274	26,373
13	1,903,890	1	506	40,038	993,922	9,598,673	40,816,089	82,606,576	82,606,576	40,816,089	9,598,673	993,922
14	7,204,874	1	616	58,955	1,813,104	22,313,159	123,919,688	336,242,252	466,659,024	336,242,252	123,919,688	22,313,159
15	27,394,666	1	741	84,595	3,161,438	48,479,302	343,116,501	1,212,929,807	2,252,676,080	2,252,676,080	1,212,929,807	343,116,501
16	104,592,937	1	882	118,721	5,305,344	99,443,287	878,332,642	3,950,577,893	9,540,203,060	12,756,460,434	9,540,203,060	3,950,577,893
17	400,795,844	1	1,040	163,426	8,615,301	194,158,877	2,101,617,914	11,788,730,647	36,159,880,264	62,793,912,275	62,793,912,275	36,159,880,264
18	1,540,820,542	1	1,216	221,173	13,597,154	363,234,599	4,742,584,436	32,609,407,748	124,582,102,308	274,438,170,936	356,238,273,248	274,438,170,936
19	5,940,738,676	1	1,411	294,839	20,930,653	654,689,624	10,168,537,421	84,420,978,408	395,042,625,208	1,082,576,666,561	1,781,181,487,071	1,781,181,487,071
20	22,964,779,660	1	1,626	387,759	31,516,302	1,141,991,891	20,843,326,708	206,179,417,105	1,164,668,766,352	3,905,398,277,399	7,986,377,556,212	10,119,349,228,496

We enumerate the fixed polyominoes from a given number of cubes, then calculate the set of valid colored polyominoes that can be generated from a given set of MMCs. We determine the shortest movement sequences to generate all reachable polyominoes from a given initial configuration. For each polyomino, we analyze the fraction of starting configurations for which it is reachable and the number of moves required to construct it.

#### A. Enumeration of fixed polyominoes

To enumerate fixed polyominoes, we implemented the method used by Redelmeier in [27]. We use a variant of this algorithm to enumerate colored polyominoes constructed from MMCs. Because the magnets in these cubes define a coordinate system, we enumerate all polyominoes with magnetic moments pointing in the  $+y$  direction. The algorithm works by recursively generating all cubes up to a given size  $n$ . We start with the leftmost cube of the bottom row, placed at the origin  $(0, 0)$ . For a given configuration with  $k$  cubes, the algorithm generates a new configuration of size  $k + 1$  by adding a cube connected to the polyomino. We maintain a list of the adjacent cubes,  $list\_adj$ , and a list of which adjacent cubes have been selected,  $poly$ , for each recursive call. In the initial call, the list of adjacent cubes,  $list\_adj$ , consists of the origin  $(0, 0)$ , the cube above the origin  $(0, 1)$ , and the cube to the right of the origin  $(1, 0)$ . We set  $poly[0] = 0$ . At each recursive call, if  $k \equiv n$ , the procedure returns. Otherwise, a recursive call is made for each cube in  $list\_adj$  greater than the last cube in  $poly$ . For each of these calls, the cube is added to  $poly$ , and any cubes adjacent to the new cube are appended to  $list\_adj$  if they are not already in  $list\_adj$ . To avoid generating the same cube more than once, cubes are only added if they are above the origin, or in the same row to the right of the origin:

$$\{(x, y) \mid (y > 0) \text{ or } (y \equiv 0 \text{ and } x \geq 0)\} \quad (2)$$

#### B. Enumeration of valid colored polyominoes from a set

To count the number of valid colored polyominoes from a set of colored cubes, we modify the previous algorithm.

We include the coloring information in  $poly$ . Before each recursive call, we check if the new cube can be colored in the given color. A check is successful if there are sufficient unused cubes of the color, and if placing the cube does not violate any of the magnetic-assembly rules. If the check is successful, a recursive call is performed. Fig. 2 top left shows that for  $n = 3$  cubes, 6 fixed polyominoes can be enumerated. Using a supply with one cyan and two magenta cubes produces more polyominoes than one brown and two magenta cubes. However, using three colored cubes enables constructing even more colored polyominoes.

Table I shows the number of fixed polyominoes that can be enumerated with up to  $n = 20$  cubes. It also lists the number of valid polyominoes with magenta and cyan cubes that can be constructed by coloring them with up to 20 cyan cubes. With zero to two magenta cubes, the number of valid polyominoes is less than the number of fixed polyominoes ( $C_{n,i}$  for  $i = 0, 1$  or  $2$ ). This is because two magenta or two cyan cubes can only be connected in series (with arrows aligned tip-to-tail). However, a more extensive set of polyominoes with different shapes and orientations can be constructed when the fraction of magenta cubes is increased. The largest variety is possible when  $i = \lfloor \frac{n}{2} \rfloor$ . The top right corner of Table I shows examples of valid colored polyominoes.

#### C. Self-assembly algorithm

We provide a low-fidelity motion model that can compute reachable polyomino configurations and the shortest movement sequences for a set of MMCs from an initial configuration. We assume that all modules move at the same speed in the same direction, unless they encounter a fixed obstacle. Without loss of generality, we limit the movement directions to north, east, south, and west.

Fig. 3 shows an example of all the valid colored polyominoes can be generated with 4 different cube designs. The initial configuration and the details of the movements are shown on the right. Underneath each polyomino is listed the shortest step sequence to construct it. At each

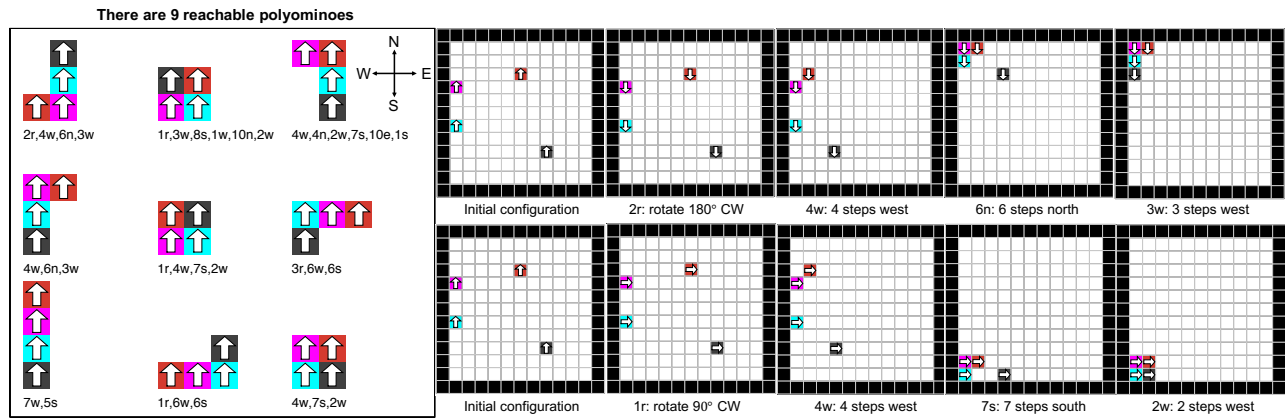


Fig. 3. **Left:** The self-assembly result for an arbitrary initial configuration of four cubes with different designs. **Right:** Details of the movements.

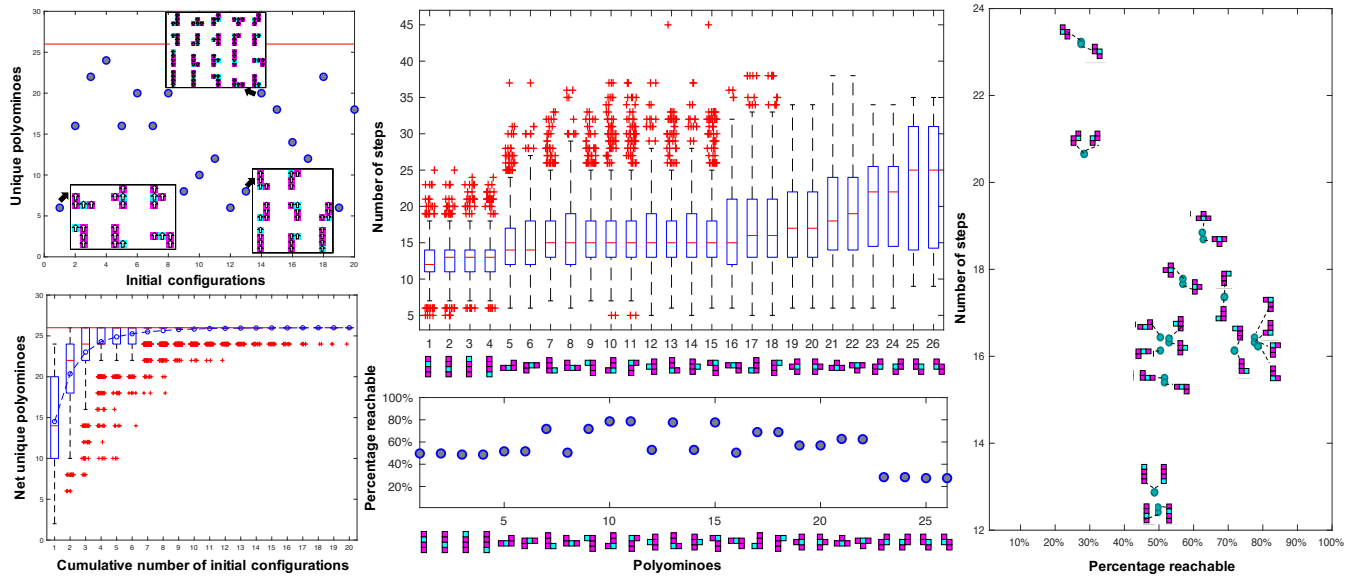







Fig. 4. **Top Left:** The number of polyominoes that can be made with 1 cyan and 3 magenta cubes from random starts. The red line is the maximum number of possible configurations (26). This test was repeated for 1000 trials, and analyzed in the remaining plots. **Bottom Left:** Cumulative number of unique reachable polyominoes. Red + signs show outliers. **Middle Top:** Total number of steps to construct each polyomino (when the polyomino is reachable). **Middle Bottom:** Frequency results showing how often each polyomino is reachable. **Right:** Scatter plot of percentage reachable vs. number of steps.

step, we could move one unit length in the four cardinal directions  $\{n, e, s, w\}$  or rotate  $\{r\}$  counterclockwise (CCW) or clockwise (CW) a quarter-turn. We prune this search by only allowing rotations if no translation moves have been made and by only performing CW rotations. For example, in this shorthand, “2r, 4w, 6n” means rotate 180° CW followed by four unit moves west, and then six unit moves north. We used a breadth-first search (BFS) algorithm to discover these reachable configurations. The root of the search is the initial configuration, and we maintain a list of all relative configurations that have been reached. A *relative configuration* is represented by rotating the coordinate frame so that the magnetic north points up and then translating all cubes. To further prune the tree, we only switch direction if the relative configuration of the cubes changes, and we terminate search branches if the present configuration has occurred before. When the relative configuration changes, we call this an *intermediate configuration*. Intermediate configurations occur when at least one cube (but not all cubes) strikes an

obstacle. When this occurs, the new relative configuration is compared to the list and is only appended if it is unique. After the polyomino is assembled, we compare the paths taken to save the shortest step sequence to construct the structure.

The number of reachable polyominoes depends on the initial configuration. For a given number of magenta and cyan cubes, a finite number of colored polyominoes can be generated (see Table I), but some may be unreachable from an arbitrary initial configuration. Different initial configurations usually generate different numbers of reachable polyominoes. Fig. 4 top left shows examples of 20 random initial configurations. For each configuration, the number of unique reachable polyominoes was calculated. Three black boxes show the valid reachable polyominoes that can be generated from three initial configurations. However, from none of these 20 configurations could we construct every one of the 26 valid colored polyominoes (see Table I). If the desired polyomino is unreachable from a given initial configuration, one could repeatedly generate new random ini-

TABLE II. NUMBER OF FIXED POLYUBES  $A_{n,3D}$ , WHERE  $n$  IS THE NUMBER OF CUBES. ROW MAXIMUM IN ORANGE. WITH MMC-R<sub>3D</sub> AND MMC-B<sub>3D</sub>,  $C_{n,i}$  IS THE NUMBER OF COLORED POLYUBES WITH  $i$  RED CUBES AND  $n$  TOTAL CUBES.

$n$	$A_3(n)$	$C_{n,0}$ (with 0 red cubes)	$C_{n,1}$ (with 1 red cube)	$C_{n,2}$ (with 2 red cubes)	$C_{n,3}$ (with 3 red cubes)	$C_{n,4}$ (with 4 red cubes)	$C_{n,5}$ (with 5 red cubes)	$C_{n,6}$ (with 6 red cubes)	$C_{n,7}$ (with 7 red cubes)	$C_{n,8}$ (with 8 red cubes)
1	1	1	1							
2	3	1	6	1						
3	15	1	25	25	1					
4	86	1	76	228	76	1				
5	534	1	188	1,322	1,322	188	1			
6	3,481	1	404	5,745	12,764	5,745	404	1		
7	23,502	1	794	20,407	86,394	86,394	20,407	794	1	
8	162,913	1	1,472	62,532	456,712	855,148	456,712	62,532	1,472	1
9	1,152,870	1	2,614	171,452	2,008,012	6,349,175	6,349,175	2,008,012	171,452	2,614
10	8,294,738	1	4,482	431,506	7,651,944	38,050,258	63,779,954	38,050,258	7,651,944	431,506
11	60,494,549	1	7,456	1,015,046	26,019,733	192,891,333	503,439,919	503,439,919	192,891,333	26,019,733
12	446,205,905	1	12,074	2,260,876	80,665,094	854,490,806	3,291,665,860	5,106,180,788	3,291,665,860	854,490,806
13	3,322,769,321	1	19,081	4,813,494	231,730,812	3,387,693,736	18,482,785,142	42,090,555,948	42,090,555,948	18,482,785,142
14	24,946,773,111	1	29,488	9,864,029	624,652,660	12,240,460,603	91,492,419,452	293,391,588,337	429,795,275,568	293,391,588,337
15	188,625,900,446	1	44,642	19,557,394	1,595,479,330	40,884,804,683	407,278,041,600	1,779,496,771,333	3,659,031,289,311	3,659,031,289,311
16	1,435,074,454,755	1	66,308	37,665,527	3,891,150,962	127,677,329,720	1,655,859,431,014	9,595,622,196,073	26,786,720,783,388	37,549,711,897,172

tial configurations until the polyomino is reachable. Rapidly rotating the magnetic field is one way to separate and scramble the cubes into new configurations.

To test the feasibility of this, we ran 1000 trials using one cyan and three magenta cubes. Fig. 4 bottom left shows the net unique polyominoes that can be constructed after a given number of configurations. The median number of reachable polyominoes from the first start is 14. With two restarts, it is possible to cover on average 20.28 of the 26 possible polyominoes configurations. In 999 out of 1000 trials, all 26 polyominoes were reachable after 20 accumulated configurations. The middle top figure shows the number of steps needed to construct each polyomino (if the polyomino is reachable) over 1000 trials. For these trials, we only counted translation steps and did not count rotation steps because translations require multiple changes to the magnetic field. The middle bottom figure shows the percentage reachable results for each polyomino. Icons at the bottom of these figures show each valid polyomino. I-shapes require on average the fewest steps to form. L-shapes with a cyan cube in the corner are reachable most often (the highest frequency is 786 out of 1000 trials). Z-shapes are harder to make because they require assembly in a specific temporal order (moving all cubes to give them the same  $y$  coordinate, so to make a Z-shape, the motion must be stopped before all cubes reach the boundary). Z-shapes also require on average the most steps to form (see Fig. 4 right).

#### IV. GENERATE ALL POSSIBLE POLYUBES IN 3D

A *polycube* is a three-dimensional polyomino constructed by cubes attaching face to face. Each cube is represented by an integer tuple  $(x, y, z)$ . Cubes 1 and 2 are adjacent if  $|x_1 - x_2| + |y_1 - y_2| + |z_1 - z_2| = 1$ . Polycubes can be enumerated in two ways, depending on whether different orientations are counted as one polycube or two. Two *free polycubes* are considered distinct if they have different shapes, but are not 3D rotations of each other. Two *fixed polycubes* are

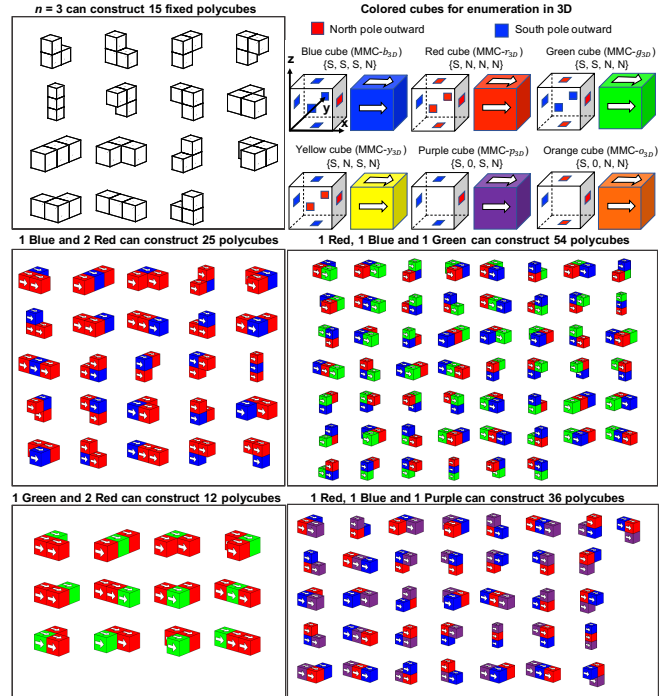


Fig. 5. Enumeration of colored cubes in 3D. The composition of cube types determines the number of polycubes that can be made. The white arrow indicates the direction of south to north magnetic pole.

considered equivalent if one can be transformed into the other by a translation. The number of fixed three-dimensional polycubes of size  $n$  is denoted by  $A_{n,3D}$ .

#### A. Enumeration of fixed polycubes

As with the enumeration of polyominoes in 2D, we start with the leftmost cube of the bottom row and place it at the origin  $(0, 0, 0)$ . In the initial call, the list of adjacent cubes, *list\_adj*, consists of the origin  $(0, 0, 0)$ , the cube to the right of the origin  $(1, 0, 0)$ , the cube to the back of the origin  $(0, 1, 0)$ , and the cube on the top of the origin  $(0, 0, 1)$ , we set  $poly[0] = 0$ . To avoid double-counting polycubes, cubes



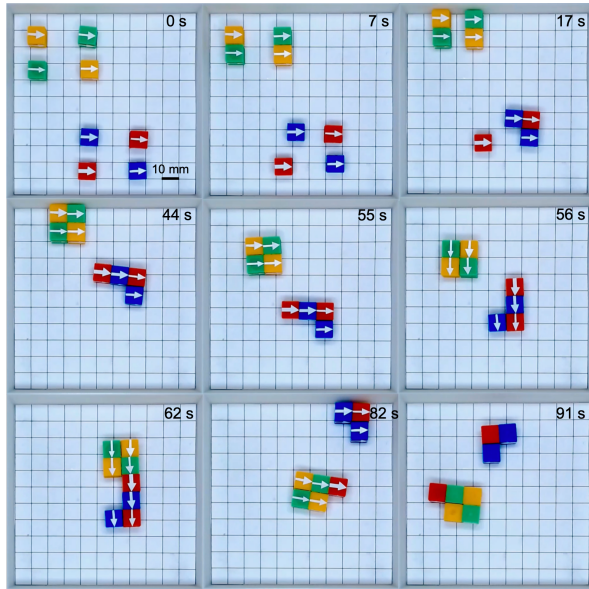


Fig. 8. 2D self-assembly and disassembly behavior of modular subunits with eight cubes.

of enumeration of valid colored polyominoes and polycubes.

## V. EXPERIMENTAL SETUP AND RESULTS

A large-scale nested triaxial Helmholtz coil system was used to conduct experiments. This system was designed parametrically to create uniform magnetic fields in  $x$ ,  $y$ , and  $z$ . Each coil pair is connected to its own programmable power supply which is controlled by a National Instruments data acquisition (DAQ) board. The power supplies generate sinusoidal outputs to the coils, which in turn creates a uniform rotating magnetic field with user-specified magnitude and frequency. These signals are controlled using a customized C++ program. The 3D magnetic field vector produced from the system is represented by

$$\mathbf{B} = \begin{bmatrix} B_x \\ B_y \\ B_z \end{bmatrix} = \begin{bmatrix} A \cos(\alpha) \cos(\theta) \\ A \cos(\alpha) \sin(\theta) \\ A \sin(\alpha) \end{bmatrix}, \quad (4)$$

where  $\mathbf{B}$  is the applied magnetic flux density,  $B_x$ ,  $B_y$ , and  $B_z$  are the three-dimensional components along  $x$ ,  $y$  and  $z$ -axes respectively,  $A$  is the amplitude,  $\alpha$  is the pitch angle, and  $\theta$  is the yaw angle. Individual cubes that have a volume of  $1\text{cm}^3$  were designed using a CAD software (Onshape) and printed using polylactic acid (PLA) on a 3D printer (Ultimaker 2 Extended+). A MATLAB program collected magnetic field settings throughout the experiment and recorded assembly behavior of modular subunits with a digital camera.

A magnetic flux of 10mT was enough to actuate the modular cubes and achieve successful assembly. Pivot walking motion was used to actuate individual modular cubes with precise motion, following predetermined paths to create a target assembly. When the arrows on top faces of the modular cubes are aligned side-by-side, this is defined as a parallel assembly. When the arrows are aligned tip-to-tail, this is defined as a serial assembly. The self-assembly is caused by the magnetic attraction force generated from

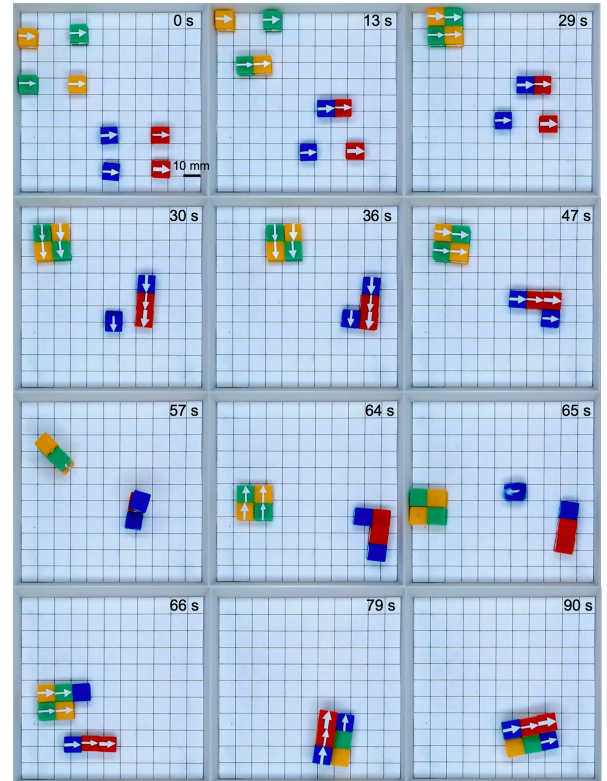


Fig. 9. 3D self-assembly and disassembly behavior of modular subunits with eight cubes.

embedded permanent magnets in the modular cubes when they are moved close to each other. Fig. 8 shows 2D self-assembly and disassembly behavior of modular subunits for eight cubes. Starting with two groups of modular cubes, with an equal number of modular cubes in each group, serial and parallel assembly were explored to form square- and J-shapes (at 44s). However, the self-assembly configuration depends on the motion path taken (i.e., parallel assembly or serial assembly) and the choice of subunits. From 44s to 55s, the assembled structures could be moved downwards by pivot walking, like an individual modular cube. From 55s to 56s, the sub-assemblies were rotated  $90^\circ$  CW by changing the direction of the static magnetic field. The sub-assemblies could then be moved right or left to bring them into close proximity. The sub-assemblies were then joined to create a large 9-shaped structure (at 62s). Then, it was disassembled into two different shapes (at 82s), with a rapid  $90^\circ$  CCW rotational magnetic torque. The disassembly occurred at the weakest magnetic joint in the structure. The modular structures can also be moved in the workspace using the rolling motion [16] which allows flipping the structures (at 91s).

Fig. 9 shows a representative 3D construction sequence using global magnetic control. A 3D self-assembly was performed following a 2D self-assembly to create a pair of sub-assemblies. Starting with a similar configuration as Fig. 8, but choosing a different motion path in the 2D self-assembly process formed an J-shape and a square-shape with different cube orderings at 36s. The sub-assemblies were rotated CW (at 30s) and CCW (at 47s) for movement in

different directions. Once 2D structures were formed with pivot walking motion followed by 2D self-assembly, the sub-units can be further joined in 3D by using rolling motions. The rolling motion was achieved by applying continuous rotational magnetic torque on the modular structures about a fixed axis until the target location was reached (from 57s to 66s). While the sub-assemblies were rolled to bring them in close proximity, a blue modular cube in the J-shaped structure was disassembled (at 65s). The blue cube reattached to the square-shaped structure (at 66s) which resulted in an unplanned reconfiguration. This spontaneous disassembly and reconfiguration could have benefits, but could also be avoided with improved control. Once the reconfigured sub-units move into close proximity, they self-assembled to create a two layered 3D structure (at 79s). This 3D structure was also actuated in the workspace with the pivot walking motion (from 79s to 90s).

## VI. CONCLUSION

This paper describes the 2D and 3D configurations of modular cubes with magnetic faces controllable by a global magnetic field. Experimental results demonstrate the self-assembly and disassembly behavior of magnetic modular cubes in 2D and 3D. Computational modeling enumerates the set of possible polyominoes and polycubes from a set of modular cubes. The 2D motion planner computes the shortest movement sequences to generate all reachable polyomino configurations.

Future work will focus on 3D planning, in particular making a high-fidelity simulator for motion planning. It would be interesting to calculate the number of valid colorings of a given polycube as a function of the supply of colored cubes. During the enumeration process one could also catalog useful configurations, ranking them on their mechanical stability, fracture modes, or magnetic profile in addition to their shape.

## REFERENCES

- [1] J. W. Romanishin, K. Gilpin, and D. Rus, "M-blocks: Momentum-driven, magnetic modular robots," in *IROS*. IEEE, 2013, pp. 4288–4295.
- [2] S. Tasoglu, C. Yu, H. Gungordu, S. Guven, T. Vural, and U. Demirci, "Guided and magnetic self-assembly of tunable magnetoceptive gels," *Nature Communications*, vol. 5, no. 1, pp. 1–11, 2014.
- [3] H. Xie, M. Sun, X. Fan, Z. Lin, W. Chen, L. Wang, L. Dong, and Q. He, "Reconfigurable magnetic microrobot swarm: Multimode transformation, locomotion, and manipulation," *Science Robotics*, vol. 4, no. 28, 2019.
- [4] W. Saab, P. Racioppo, and P. Ben-Tzvi, "A review of coupling mechanism designs for modular reconfigurable robots." *Robotica*, vol. 37, no. 2, pp. 378–403, 2019.
- [5] R. Pfeifer, M. Lungarella, and F. Iida, "Self-organization, embodiment, and biologically inspired robotics," *Science*, vol. 318, no. 5853, pp. 1088–1093, 2007.
- [6] K. Tomita, S. Murata, H. Kurokawa, E. Yoshida, and S. Kokaji, "Self-assembly and self-repair method for a distributed mechanical system," *IEEE Transactions on Robotics and Automation*, vol. 15, no. 6, pp. 1035–1045, 1999.
- [7] J. Balanza-Martinez, A. Luchsinger, D. Caballero, R. Reyes, A. A. Cantu, R. Schweller, L. A. Garcia, and T. Wylie, "Full tilt: Universal constructors for general shapes with uniform external forces," in *Proceedings of the Thirtieth Annual ACM-SIAM Symposium on Discrete Algorithms*. SIAM, 2019, pp. 2689–2708.
- [8] J. Balanza-Martinez, T. Gomez, D. Caballero, A. Luchsinger, A. A. Cantu, R. Reyes, M. Flores, R. Schweller, and T. Wylie, "Hierarchical shape construction and complexity for slidable polyominoes under uniform external forces," in *Symposium on Discrete Algorithms*. SIAM, 2020, pp. 2625–2641.
- [9] A. T. Becker, S. P. Fekete, P. Keldenich, D. Krupke, C. Rieck, C. Scheffer, and A. Schmidt, "Tilt assembly: Algorithms for micro-factories that build objects with uniform external forces," *Algorithmica*, vol. 82, no. 2, pp. 165–187, 2020.
- [10] P. Keldenich, S. Manzoor, L. Huang, D. Krupke, A. Schmidt, S. P. Fekete, and A. T. Becker, "On designing 2d discrete workspaces to sort or classify polyominoes," in *IROS*. IEEE, 2018, pp. 1–9.
- [11] P. Holobut and J. Lengiewicz, "Distributed computation of forces in modular-robotic ensembles as part of reconfiguration planning," in *2017 IEEE International Conference on Robotics and Automation (ICRA)*. IEEE, 2017, pp. 2103–2109.
- [12] B. Piranda, P. Chodkiewicz, P. Holobut, S. Bordas, J. Bourgeois, and J. Lengiewicz, "Distributed prediction of unsafe reconfiguration scenarios of modular-robotic programmable matter," *arXiv preprint arXiv:2006.11071*, 2020.
- [13] A. Bhattacharjee, Y. Lu, A. T. Becker, and M. J. Kim, "Magnetically-controlled modular cubes with reconfigurable self-assembly and disassembly," *IEEE Transactions on Robotics*, 2021.
- [14] E. Al Khatib, A. Bhattacharjee, P. Razzaghi, L. W. Rogowski, M. J. Kim, and Y. Hurmuzlu, "Magnetically actuated simple millirobots for complex navigation and modular assembly," *IEEE Robotics and Automation Letters*, vol. 5, no. 2, pp. 2958–2965, 2020.
- [15] L. Rogowski, A. Bhattacharjee, X. Zhang, G. Kararsiz, H. Fu, and M. J. Kim, "Manipulation planning of magnetically actuated programmable cuboids for collaborative assembly," in *2020 IEEE/RSJ International Conference on Intelligent Robots and Systems, Las Vegas, NV, USA*, 2020.
- [16] C. Bi, M. Guix, B. V. Johnson, W. Jing, and D. J. Cappelleri, "Design of microscale magnetic tumbling robots for locomotion in multiple environments and complex terrains," *Micromachines*, vol. 9, no. 2, p. 68, 2018.
- [17] G. Aleksandrowicz and G. Barequet, "Counting d-dimensional poly-cubes and nonrectangular planar polyominoes," in *International Computing and Combinatorics Conference*. Springer, 2006, pp. 418–427.
- [18] S. Luther and S. Mertens, "Counting lattice animals in high dimensions," *Journal of Statistical Mechanics: Theory and Experiment*, vol. 2011, no. 09, p. P09026, 2011.
- [19] G. Barequet and M. Shalah, "Polyominoes on twisted cylinders," in *Proceedings of the Twenty-Ninth Annual Symposium on Computational Geometry*, 2013, pp. 339–340.
- [20] A. R. Conway, "The design of efficient algorithms for enumeration," *arXiv preprint arXiv:1610.09806*, 2016.
- [21] G. Barequet and M. Shalah, "Improved upper bounds on the growth constants of polyominoes and polycubes," *arXiv preprint arXiv:1906.11447*, 2019.
- [22] E. D. Demaine, M. L. Demaine, D. Eppstein, and J. O'Rourke, "Some polycubes have no edge-unzipping," *arXiv preprint arXiv:1907.08433*, 2019.
- [23] G. Barequet, G. Rote, and M. Shalah, " $\lambda > 4$ : An improved lower bound on the growth constant of polyominoes," *Commun. ACM*, vol. 59, no. 7, pp. 88–95, 2016.
- [24] D. Caballero, A. A. Cantu, T. Gomez, A. Luchsinger, R. Schweller, and T. Wylie, "Building patterned shapes in robot swarms with uniform control signals," in *Proceedings of CCCG*, 2020.
- [25] U. K. Cheang, F. Meshkati, H. Kim, K. Lee, H. C. Fu, and M. J. Kim, "Versatile microrobotics using simple modular subunits," *Scientific Reports*, vol. 6, p. 30472, 2016.
- [26] Y. Lu and A. T. Becker, March 2021. [Online]. Available: <https://github.com/RoboticSwarmControl/EnumeratingPolycubes/>
- [27] D. H. Redelmeier, "Counting polyominoes: yet another attack," *Discrete Math.*, vol. 36, no. 2, pp. 191–203, 1981.
- [28] L. He, X. Ren, Q. Gao, X. Zhao, B. Yao, and Y. Chao, "The connected-component labeling problem: A review of state-of-the-art algorithms," *Pattern Recognition*, vol. 70, pp. 25–43, 2017.